Signal Processing and Renewable Energy
December 2017, (pp.9-25)
ISSN: 2588-7327
eISSN: 2588-7335

A New Passive Islanding Detection Method for Distributed Generations Using Time-Frequency Transform-Based EMD-HT

Abbas Doroozi[1], Javad Olamaei [1*]

[1] Electrical Engineering Department, South Tehran Branch, Islamic Azad University, Tehran, Iran.

Abstract

This paper presents a new method based on empirical mode decomposition and Hilbert transform for detecting islanding from non-islanding events in distributed generations. In this paper, the empirical mode decomposition is used to separate out intrinsic mode functions (IMF) from non-stationary power signal disturbance waveforms. Then, the Hilbert transform applied on all the IMFs to extract the instantaneous amplitude and frequency components. The required index is extracted from the energy spectrum density of the signals that introduced as U1, U2, and U3 and we can detect islanding events with high accuracy, low cost and high speed in distributed generations.

Keywords: Distributed Generations, Empirical Mode Decomposition, Hilbert Transform, Power Spectrum Density, Power Mismatch, Islanding Detection.

1. INTRODUCTION

Participation of distributed generations (DGs) in the electrical grids has many advantages such as increased reliability, reduction in line losses, reduced dependence on fossil-fuel-based generation and so on. In addition, the grid-connected consumers can sell their extra generations to the utility. However, some of DG's challenges solved, but there is a critical issues associated with DG integration that is Islanding.

Islanding is a condition where a part of the network is isolated from the main power grid and only distributed generations feed the consumers. Although, it is not a bad thing for operation of the system, but it make some problems. Current standards such as IEEE Std 1547 suggests that the frequency and voltage of system must be within the specified range, and may be this not achieved in an island condition [1, 2].

Also, the safety of line workers is at risk when the lines that are disconnected from the main power grid are still energized by DGs. therefore it is so important that the DGs equipped with an islanding detection system.

Many studies about islanding detection have been done for synchronous and inverter based DGs. Some of methods are used for both DGs but some of them only used for

*****Corresponding Author's Email: J_olamaei@azad.ac.ir

specific type. In general, islanding detection methods divided into active, passive and communication based methods. Passive methods, only by measurement at the point of common coupling (PCC), recognize the islanding events. This is an advantage but to increase the detection accuracy, we can't rely to some system parameters, because there are other non-islanding events that produce parameters much closer to islanding events. Therefore, setting of thresholds must be wide to avoid false detection. On the other hand, this mater lead to make large non-detection zones (NDZ). In these methods, the main challenge is to select required parameters and thresholds to detecting islanding from non-islanding correctly. Some passive methods are: UV/OV, UF/OF [3-5]; Rate of change of active power [6-7]; ROCOF [8-11]; Rate of change of frequency over power [12]; Voltage and power factor change [13]; COROCOF [14]; Phase jump detection [15]; VU/THD [16-17]; VSR [18-20].

Active methods, introduce perturbation into the power system. So, by these methods, the power-quality problems appear. When the condition is non-islanding, these perturbations can't deviate desired parameters, but in the absence of the utility, perturbations deviate desired parameters and by a positive feedback, this small deviations will be amplified and at finally lead to islanding detection. The advantage of these methods over passive methods is their small Non-Detection Zones (NDZ). The main disadvantage of them is power quality problems that can lead to instability of the system. The main challenge at these methods is power quality issues. Some active methods are: Impedance detection [21-23]; Change of output power periodically [24]; APS [25]; AFD [26-29]; SMS [30-32]; Reactive power export error [33-34]; SFS [35-37]; SVS [38]; Harmonic current injection [39].

Communication based methods have high reliability but they are expensive. So, passive or active methods used in industry to reduce administrative costs.

The mentioned methods were classical methods. Recently the new passive methods based on transient signal processing modes have been introduced and have obtained good results.

One of these methods is [40] that use the wavelet transform for signal processing and apply the classifier to training the network and recognize islanding events. But wavelet transform have no application for discrete and nonlinear signals and network training is time-consuming and difficult task and requires a lot of scenarios. Another method has been introduced that is based on the Stockwell transform and extract two energy indexes for islanding detection [41]. However, this method is robust against noise and has high accuracy, but has high computational cost and they can't be used online.

So these problems impulse I to find a new islanding detection with more accuracy, lower cost, higher speed, simple computations, without inject perturbation to the network and support non-linear and discrete signals. This article propose a new passive method based-on time-frequency transform by Empirical Mode Decomposition (EMD) and Hilbert transform that has been used at signal processing. This method by using of the obtained power spectrum from intrinsic mode functions (IMFs) and instantaneous frequency (IF), can detect islanding occurrence with high accuracy. Supporting non-linear and discrete signals, more accuracy, lower cost, higher speed and simple computations that can be online, are this method advantages. In table I we compare EMD-HT with Wavelet

transform and Fourier transform. The advantages of proposed method are clearly obvious.

2. EMPIRICAL MODE DECOMPOSITION (EMD)

The EMD algorithm attempts to decompose nearly any signal into a finite set of functions, whose Hilbert transforms give physical instantaneous frequency values. These functions are called intrinsic mode functions (IMFs) [42]. The algorithm utilizes an iterative sifting process which successively subtracts the local mean from a signal. The first IMF contains the highest frequency of each event in the signal. For example a signal that contains two waveforms, one from $0 < t < t_1$ with 50 Hz and 150 Hz and another from $t_1 < t < t_2$ that contains 50 Hz and 250 Hz. The first IMF will contain the 150 Hz signal from $0 < t < t_1$ and 250 Hz from $t_1 < t < t_2$. An IMF has the following properties:

- The number of extremums and the number of zero crossings must be either equal or differ at most by one.
- At any point, the mean value of the envelope defined by the local maximum and the envelope defined by the local minimum is zero.

The sifting process is as follows:

1) Obtain envelopes defined by local minimum and minimums.
2) By cubic spline function, connect local maximums as the upper envelope and local minimums as the lower envelopes.
3) M_1 is the mean value of two envelopes. Subtract M_1 from original signal.
$$X(t) - M_1 = K_1 \quad (1)$$
4) If K1 is an IMF then K_1 is the first IMF else we suppose K_1 as the original signal and repeat steps from (1) to (3) to get the K_{11}.
$$K_1 - M_1 = K_{11} \quad (2)$$
5) After repeated up to n times, obtain K_{1n} as an IMF.
$$K_{1(n-1)} - M_{1n} = K_{1n}\,;\;\; C_1 = K_{1n} \quad (3)$$
6) Now C_1 is the first IMF that extract from original signal. Subtract C_1 from X(t).
$$X(t) - C_1 = R_1 \quad (4)$$
7) Now suppose R_1 as the original signal and repeat above steps to get the second IMF.
8) The above steps repeat q times and we obtain q IMFs from original signal.
9) This process stopped when R_q becomes small enough or a monotone function

Table 1. ***Comparison between EMD-HT with wavelet and Fourier transform.***

Type Property	**EMD-HT Transform**	**Wavelet Transform**	**Fourier Transform**
basic	Comparative	Forecast	Forecast
Frequency	Differential : local certainty	Convolution : absolute uncertainty	Convolution : absolute uncertainty
Output	Time-Frequency-Energy	Time-Frequency-Energy	Time-Frequency-Energy
Discrete signal	Yes	No	No
Non-stationary signal	Yes	Yes	No
Features extraction	Yes	Discrete : No Continuous : Yes	No
Theoretical basic	Empirical	Complete theory	Complete theory

that can not be extracted from the IMF components.

Fig. 1 shows the non-stationary power signal that includes different disturbances and extracted IMFs which were obtained by EMD.

3. HILBERT TRANSFORM

Hilbert transform is usually used to generate complex time series or analytic signal. The benefit is that by using the HT on a signal X(t), a meaningful instantaneous magnitude and frequency can be obtained as long as the signal does not have mixed frequency components. But, to achieve accurate computation of these attributes, the input signals of Hilbert transform must have zero means, in otherwise the information obtained from the Hilbert transform, may not be valid. Thus, the most important role of EMD is to prepare input signal for Hilbert transform. In [43] is expressed how to use IMFs for obtaining the instantaneous amplitude and frequency for analysis of the events occurred. The Hilbert transform of the continuous signal X(t), defined as :

$$y(t)=\int_{-\infty}^{+\infty}\frac{x(t)}{t-\tau}dt \tag{5}$$

In a simple term, the Hilbert transform of a signal, produces an orthogonal signal that is phase shifted by 90 degrees from the original signal independent of the frequency of the signal [44].

For non-stationary signals the defined frequency of sinusoidal signals isn't effective so we used instantaneous frequency (IF) that is effective in mono-component signal that be composed of a single frequency or a narrow band of frequencies. The analytical signal Z(t), obtained by HT of the signal X(t), defined as:

$$Z(t) = X(t) + jY(t) = a(t)e^{j\theta(t)} \tag{6}$$

$$a(t) = [X(t)^2 + Y(t)^2]^{\frac{1}{2}} \tag{7}$$

$$\theta(t) = arctan\left[\frac{Y(t)}{X(t)}\right] \tag{8}$$

Where $Y(t)$ is the HT of $X(t)$, $a(t)$ is instantaneous amplitude and $\theta(t)$ is instantaneous phase angle. Instantaneous frequency (IF) is rate of change of instantaneous phase angle:

$$IF = \frac{W}{2\pi} = \frac{1}{2\pi}\frac{d\theta}{dt} \tag{9}$$

By applying HT on all IMFs, we obtain corresponding analytical signal for each of them.

$$\begin{aligned} Z_1 &= IMF_1(t) + jH[IMF_1(t)] = a_1(t) + e^{j\theta_1(t)} \\ Z_2 &= IMF_2(t) + jH[IMF_2(t)] = a_2(t) + e^{j\theta_2(t)} \\ &\vdots \\ Z_n &= IMF_n(t) + jH[IMF_n(t)] = a_n(t) + e^{j\theta_n(t)} \end{aligned} \tag{10}$$

After applying HT on all IMFs, the original signal can be expressed as the follow equation:

$$X(t) = \sum a_i(t)\, e^{j\theta_i(t)} = \sum a_i(t)\exp\left(j\int w_i(t)\,dt\right) \tag{11}$$

So we can represent instantaneous amplitude and frequency as function of time and frequency. This distribution of the amplitude is well known as Hilbert amplitude spectrum or simply Hilbert spectrum [45]. Empirical Mode Decomposition with Hilbert transform is a useful and promising way for signal processing. The EMD prepare input signal for Hilbert transform to obtain the instantaneous amplitude and frequency which are two important attribute for detection and classification of power disturbances.

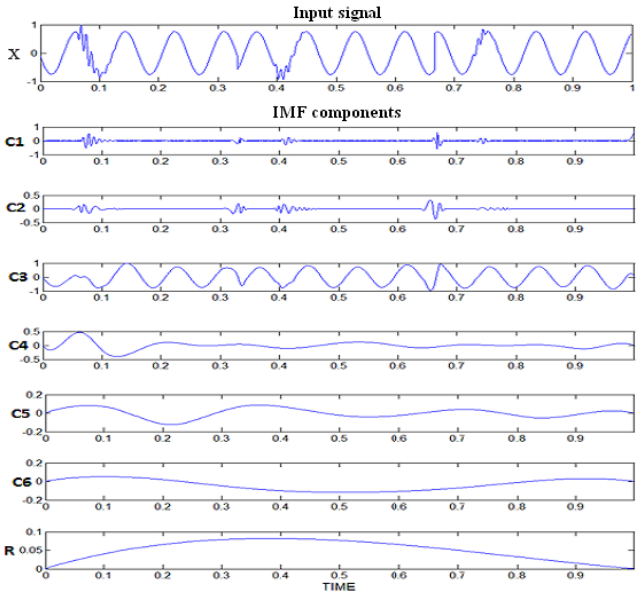

Fig. 1. Decompose X(t) to intrinsic Mode functions (IMFs).

4. SYSTEM STUDIED

The system studied for proposed method is shown in Fig. 2. The operation voltage and frequency of microgrid is 25 kV and 60 Hz. The studied system consist of 4 DG units (3 wind farms and 1 gas turbine) connected to the main supply with rated short-circuit 5000 MVA.

The voltage of each distribution lines is 25 kV and simulates as pi-section. The details of DGs, transformers, distribution lines and loads are mentioned as follows:

- Utility: rated short-circuit = 5000 MVA, f = 60 Hz, rated voltage = 120 kV.
- Distributed Generations (DGs):
  1) DG-1, DG-2, DG-3: Wind farm (6 MW) consisting of three 2 MW wind turbines. The DFIG has been considered.
  2) DG-4: gas turbine, 9 MW, 2400 V.
- Transformer TR-1: rated power = 50 MVA, rated voltage = 120/25 kV, f = 60 Hz, R_1 = 0.00375 p.u., X_1 = 0.1 p.u., R_m = 500 p.u., X_m = 500 p.u.
- Transformer TR-2, TR-3, TR-4: rated power = 7 MVA, rated voltage = 575 V/25 kV, f = 60 Hz, R_1 = 0.0008 p.u., X_1 = 0.025 p.u., R_m = 500 p.u., X_m = 500 p.u.
- Transformer TR-5: rated power = 10 MVA, rated voltage = 2.4/25 kV, f = 60 Hz, R_1 = 0.0015 p.u., X_1 = 0.03 p.u., R_m = 200 p.u., X_m = 200 p.u.
- Distribution lines: DL-1, DL-2, DL-3 and DL-4: pi-section, 20 km, rated voltage = 25 kV, rated power = 20 MVA, R_1 = 0.413 Ω/km, R_0 = 0.1153 Ω/km, L_1 = 3.32e-3 H/km, L_0 = 1.05e-3 H/km, C_1 = 5.01e-9 F/km, C_0 = 11.33e-9 F/km
- Loads: L_1 = 12 MW , 4 Mvar; L_2 = L_3 = L_4 = L_5 = 4 MW , 1 Mvar.

The relays for each DG are placed at the low voltage side to collect voltage signal for islanding detection. The simulation is carried out using the Matlab/Simulink software. The islanding and non-islanding conditions that studied in this paper, are as follows:

- Loss of load at PCC.
- Tripping of other DGs apart from target DG.
- Loss of any distribution lines.
- Sudden load change at PCC.
- Capacitor switching.
- Induction motor starting (2250 hp).
- Sudden load change on the target DG location.
- Opening of any breakers between DG and power grid.
- Events that lead to trip breakers and cause the DG to be studied is an island.

5. SIMULATION RESULTS

In this paper, the voltage signal measured at the desired DG location and decomposed throws EMD and prepared the input signal for HT and finally by using of power spectrum density of extracted signals, the islanding is detected.

For islanding evens detection, four signals are defined. Three signals U1,U2 and U3 are derived from the product of instantaneous

frequency and amplitude of the first three IMFs. The signal Ut is achieved from the sum of these three signals.

$$\begin{aligned} U_1(t) &= a_1(t) \times IF_1(t) \\ U_2(t) &= a_2(t) \times IF_2(t) \\ U_3(t) &= a_3(t) \times IF_3(t) \\ U_t(t) &= U_1(t) + U_2(t) + U_3(t) \end{aligned} \quad (12)$$

After calculating the Power Spectrum Density (P.S.D) of these signals (in terms of decibel watt per hertz (dbw/hz)), by setting a threshold, islanding occurrence is detected. One of the most difficult diagnoses is the capacitor switching events. The changes that occur in this event are so similar to islanding events. For detecting this event, U1 and U2 are used. Capacitor switching make spikes at these two signals but in islanding events there isn't this trend. The flowchart for the proposed scheme for islanding detection is given in Fig. 3.

Fig. 4 and Fig. 5 shows the results at DG-2 for islanding condition with 0% of power mismatch. As the figures show, thresholds of the power spectrum density indicate the occurrence of the islanding correctly.

Fig. 6 shows the results at DG-2 for non-islanding condition (sudden load change at the PCC). As is obvious from figures, the desired thresholds, according to the presented flowchart recognize non-islanding event correctly.

Fig. 7 shows the results at DG-1 for islanding condition with 0% of power mismatch. Also in this scenario by proposed method and thresholds (according to presented flowchart), islanding event is detected correctly. According to the IEEE Std 1547, maximum time to detect islanding is 2 second and if a relay cannot detect in this period of

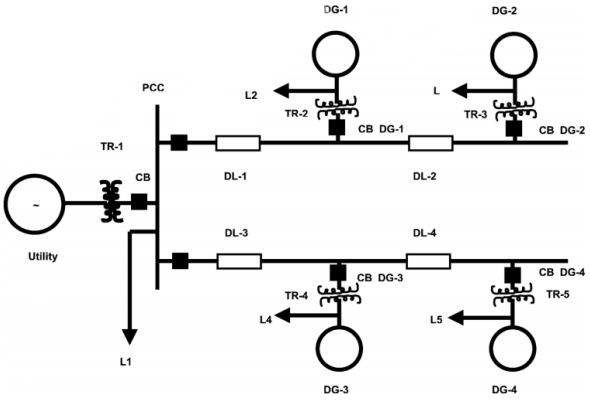

Fig. 2. System studied for the proposed method.

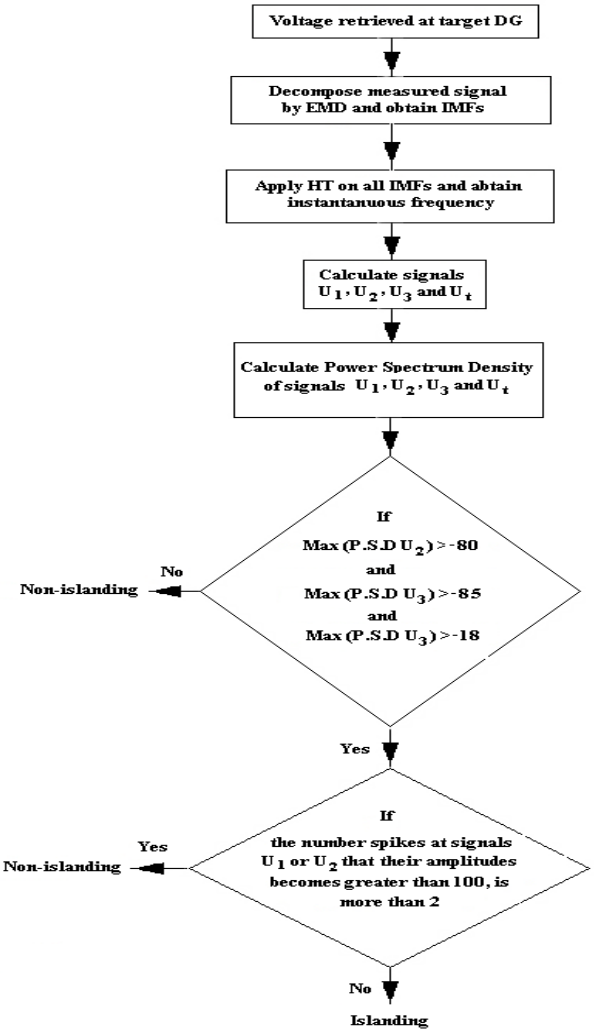

Fig. 3. Flowchart for the proposed scheme for islanding detection.

time, it has failed. The proposed method sampling frequency is 20 kHz on a base fre-

quency of 60 Hz and only uses 324 sampling data to islanding detection. This means that the response time of the relay is less than one cycle. So the proposed method has a high speed and is suitable.

Fig. 8 shows the results at DG-1 for non-islanding condition (DG-2 tripped). The results, confirm the validity and accuracy of the proposed method.

Capacitor switching, create the changes that are so similar to islanding events. For detecting this event, U1 and U2 are processed. If the number of spikes that their amplitudes are greater than 100, is more than 2 number, the occurrence event is non-islanding, because in islanding events there isn't this trend.

FIG. 9 shows the results at DG-1 for 1Mvar capacitor switching. We can see several spikes with great amplitude at signals U1 and U2. Thus by using of proposed flowchart at

Fig. 3, the capacitor switching is recognized from other events.

To verify the validation of this matter, 200 kvar capacitor switching is performed at DG-3 and the results are shown at Fig. 10. It is obvious from figures witch in the U1 there is five spikes that four of themes have amplitude greater than 100.

Fig. 11 shows the results at DG-4 for direct starting of the induction motor with 2.4 kV and 2250 hp at the PCC. The active and reactive powers at the PCC are shown in Fig. 12. It is observable at starting duration time that is about three second, huge reactive power derived from the grid suddenly and lead to voltage sag but the proposed islanding detection method yet successfully recognize correctly non-islanding events.

The complete statistics of the power spectrum density and corresponding total P.S.D at DG-2 and DG-4 and DG-1 are depicted in Tables II and III and IV for different active and reactive power mismatch respectively. The results of the paper [46], confirm the validation of this method.

Tables V and VI shows the results of [46] that is based on Wavelet Singular Entropy.

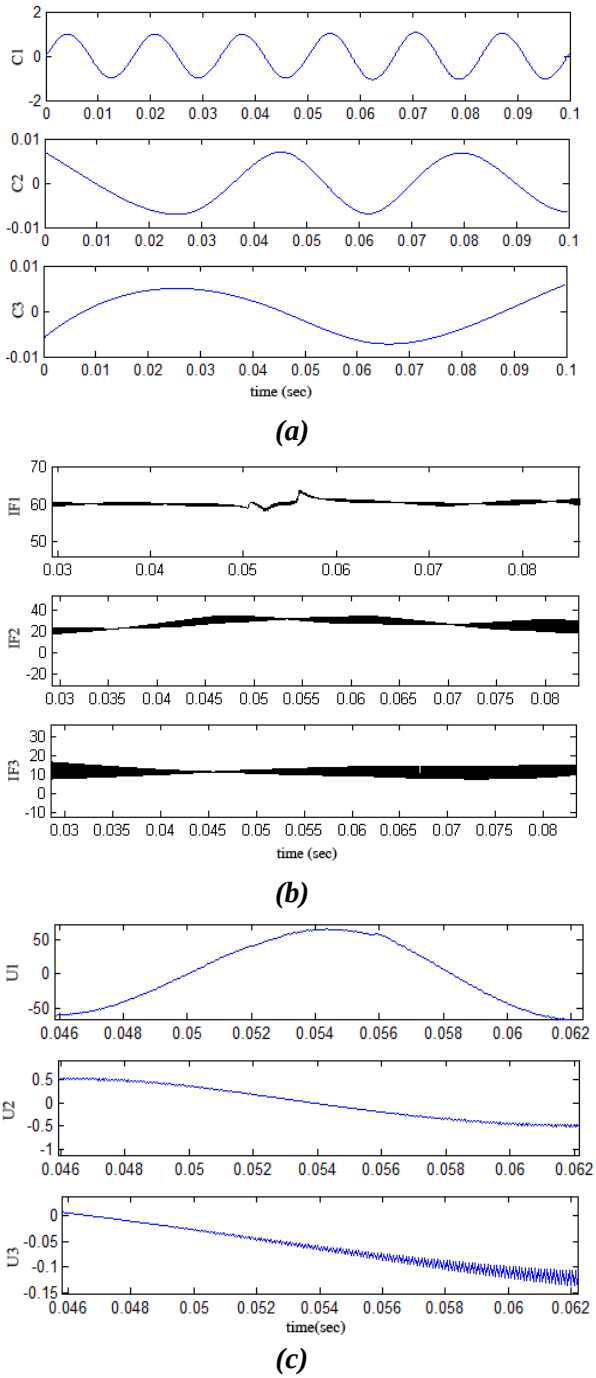

Fig. 4. The first three IMFs at DG-2 with power mismatch 0%. (b) Instantaneous frequency of IMFs. (c) Defined signals U1, U2 and U3.

In the paper [46] the WSEI index which is derived from Shannon entropy of the first four detailed coefficients of Wavelet Transform, is used to islanding detection by a threshold (greater than 2). But the capacitor switching that is one of the difficult diagnoses in islanding detection, were not considered at none scenario. The other events which were not attend to it, is direct induction motor starting that derive high power from the network and lead to voltage sag.

In the proposed method this scenarios is performed and aforementioned results shows the correct islanding detection.

According to the obtained results at the [47], the accuracy of the proposed method and other methods has been compared in tables VII and VIII.

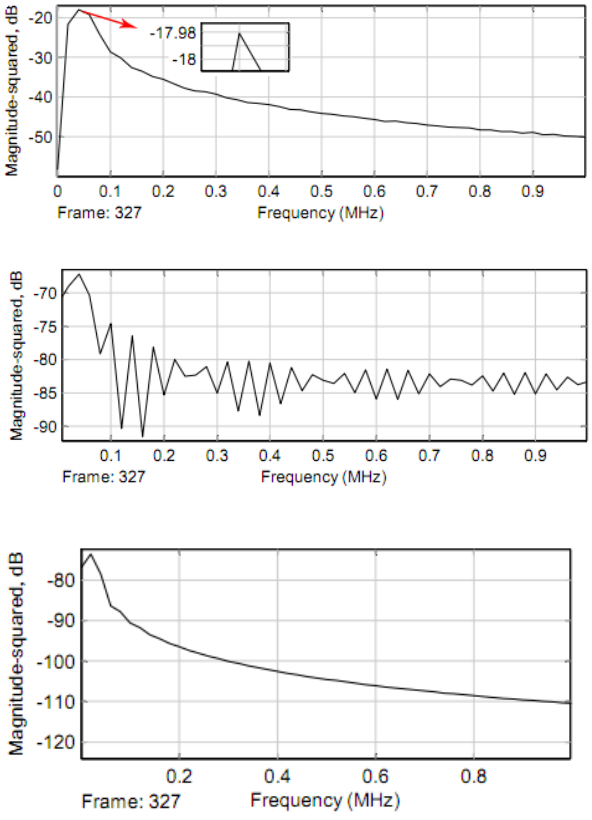

Fig. 5. Islanding at DG-2 with 0% power mismatch (a) P.S.D of the Ut. (b) P.S.D of the U2. (c) P.S.D of the U3.

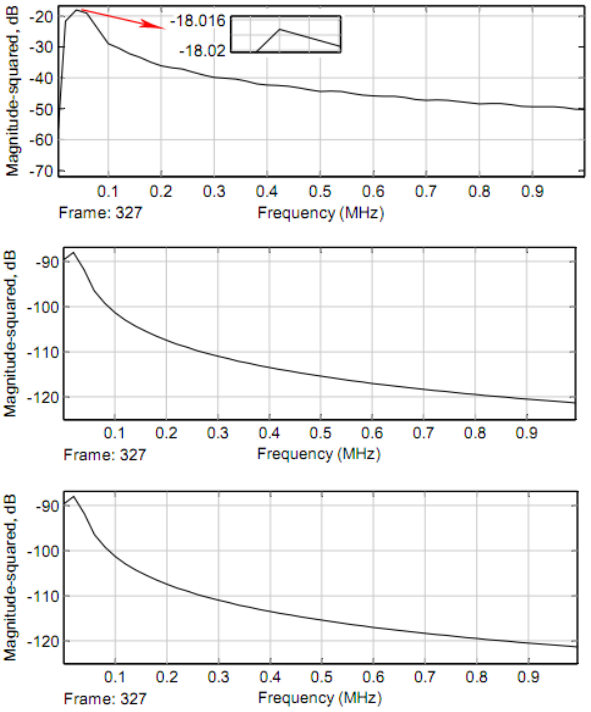

Fig. 6. Non-islanding, sudden load change at PCC (a) P.S.D of the Ut. (b) P.S.D of the U2. (c) P.S.D of the U3

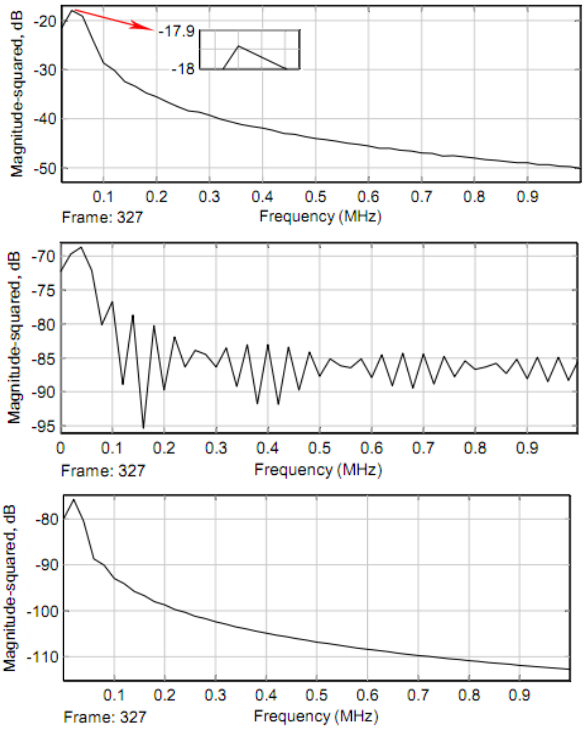

Fig. 7. Islanding at DG-1 with 0% power mismatch (a) P.S.D of the Ut. (b) P.S.D of the U2.(c) P.S.D of the U3.

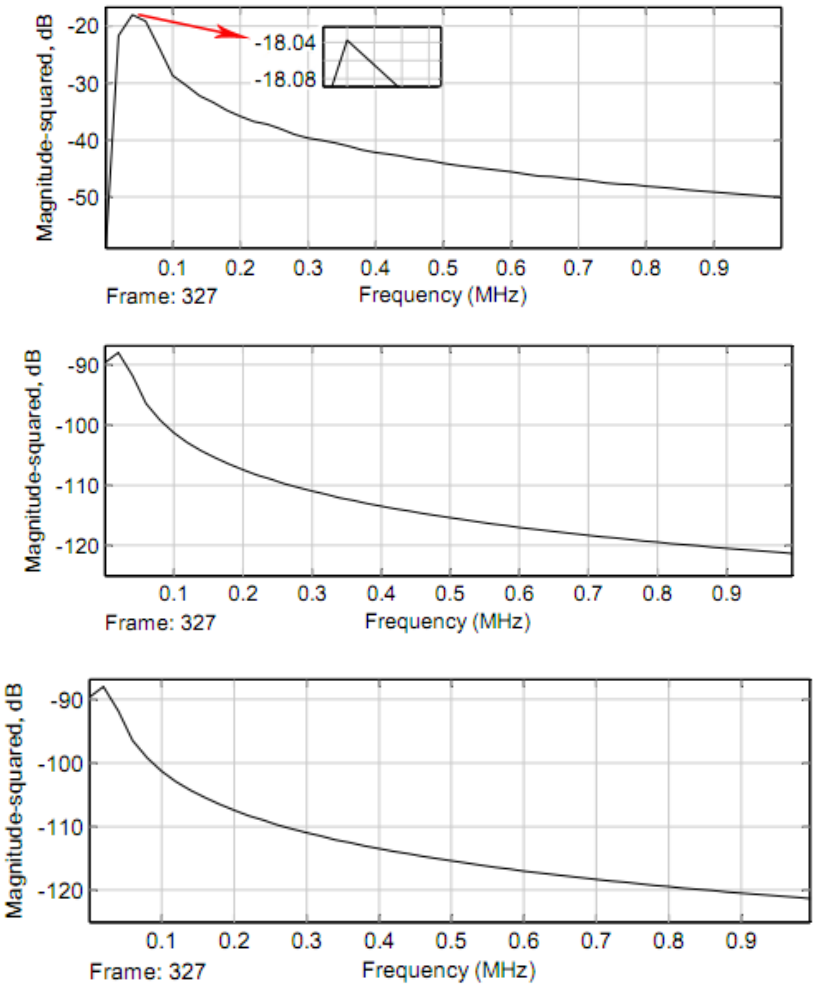

Fig. 8. Non-islanding event (DG-2 tripped) at DG-1 (a) P.S.D of the Ut. (b) P.S.D of the U2. (c) P.S.D of the U3.

Table 2. ***Effective power spectrum density for different power mismatch during islanding and non-islanding conditions at target DG-2.***

	Events	P.S.D U_1	P.S.D U_2	P.S.D U_3	P.S.D U_t
Islanding	0% Active Power mismatch	-17.95	-67.1	-73	-17.98
	5% Active Power mismatch	-17.92	-62.7	-71.6	-17.98
	5% Active and Reactive Power mismatch	-17.92	-59.08	-76.81	-17.8
Non-Islanding	Load switching at PCC	-18.05	-87.96	-87.96	-18.05

Table 3. Effective power spectrum density for different power mismatch during islanding and non-islanding conditions at target DG-4.

EVENTS		P.S.D U_1	P.S.D U_2	P.S.D U_3	P.S.D U_t
Islanding	0% Active Power mismatch	-9.5	**-72.76**	**-83.9**	**-9.5**
	5% Active Power mismatch	-31.6	**-8.65**	**-31.77**	**-8.15**
	80% Active Power mismatch	-43.4	**-18.05**	**-34.2**	**-16.09**
	0% Reactive Power mismatch	-9.75	**-72.79**	**-83.98**	**-9.53**
	10% Reactive Power mismatch	-9.35	**-52.5**	**-83.9**	**-9.5**
	60% Reactive Power mismatch	-35	**-36.5**	**-7**	**-6.95**
Non-Islanding	Load switching at DG-1	-18.07	-87.96	-87.96	-18.07
	DG-1 tripped	-18.19	-87.96	-87.96	-18.19
	Load switching at PCC	-27.05	-19.28	-39.05	-20.92
	DG-2 tripped	-18.04	-87.96	-87.96	-18.04

Table 4. ***Effective power spectrum density for different power mismatch during islanding and non-islanding conditions at target DG-1.***

EVENTS		P.S.D U_1	P.S.D U_2	P.S.D U_3	P.S.D U_t
Islanding	0% Active Power mismatch	-17.96	**-68.43**	**-75.4**	**-17.98**
	10% Active Power mismatch	-17.84	**-59.3**	**-69.3**	**-17.93**
	80% Active Power mismatch	-6.75	**-36.36**	**-52.8**	**-6.5**
	5% Reactive Power mismatch	-17.8	**-59.24**	**-77.38**	**-17.87**
Non-Islanding	DG-2 tripped	-18.05	-87.96	-87.96	-18.05

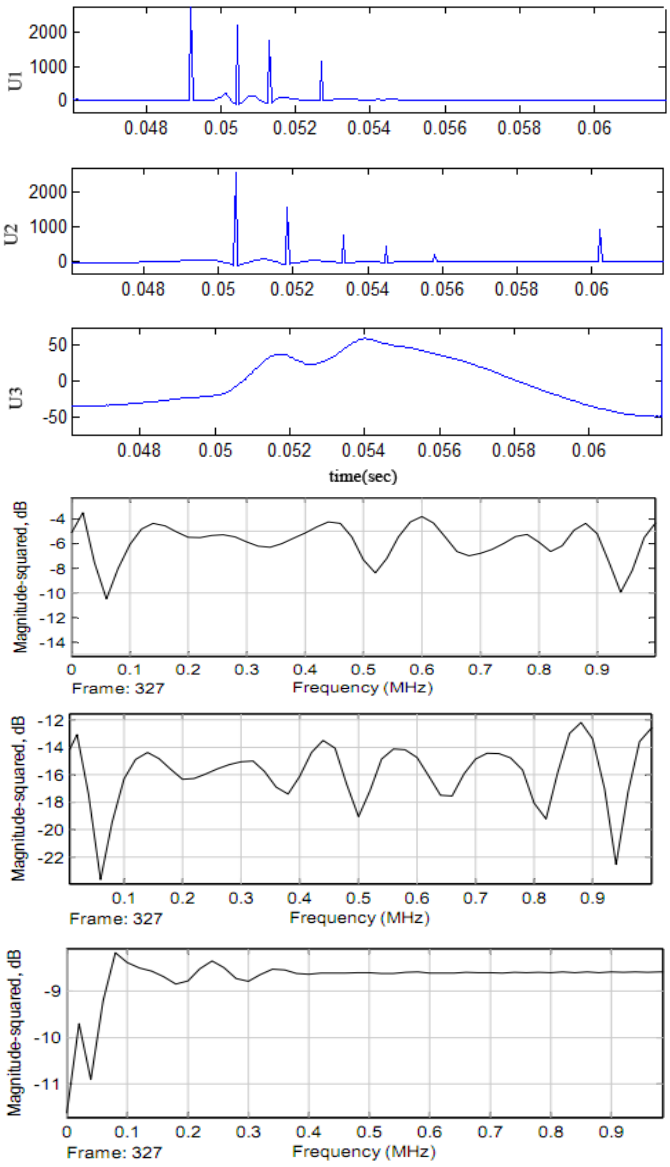

Fig. 9. 1Mvar capacitor switching at DG-1 (a) Defined signals U1, U2 and U3. (b) P.S.D of the Ut. (c) P.S.D of the U2. (d) P.S.D of the U.

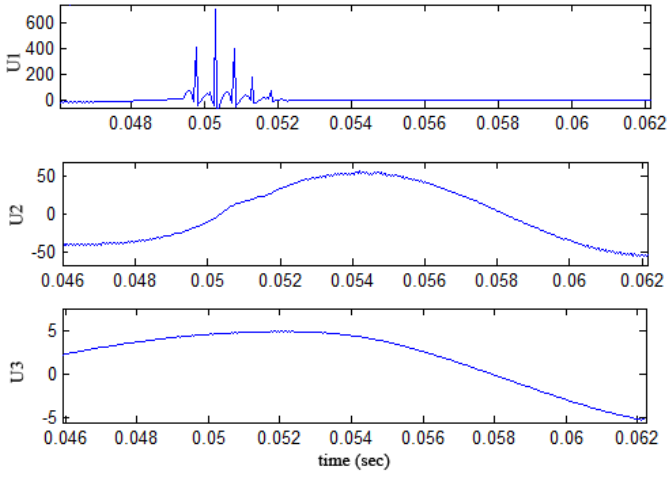

Fig. 10. Signals U1, U2 and U3 at DG-3 with 200 kvar capacitor switching

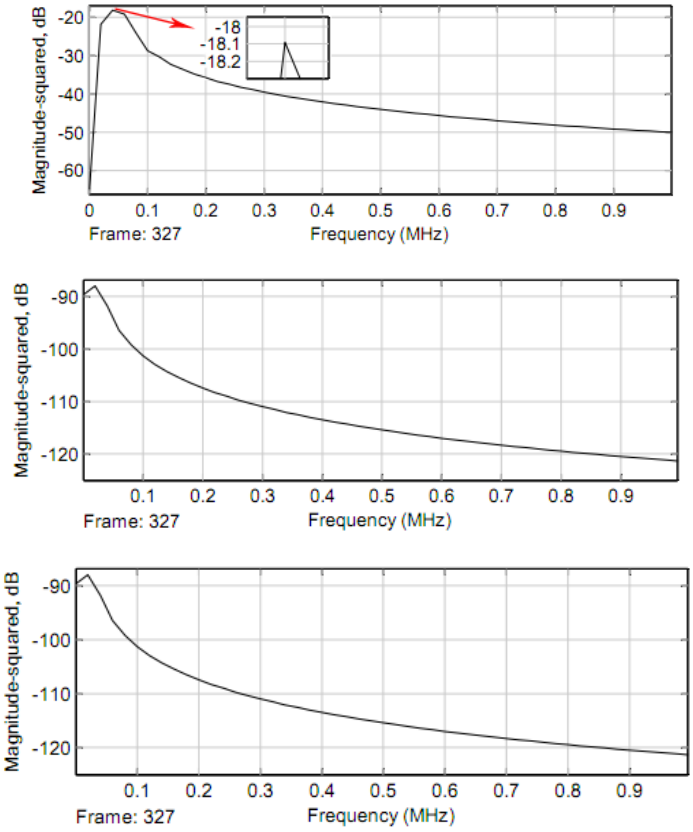

Fig. 11. Non-islanding event (motor starting) at DG-4 (a) P.S.D of the Ut. (b) P.S.D of the U2. (c) P.S.D of the U3.

Table 5. ***Effective singular values and WSEI for active power mismatch during islanding and non-islanding conditions at target DG-4 [46].***

EVENTS		Phase	λ_1	λ_2	λ_3	λ_4	WSEI
Islanding	0% Power mismatch	a	10.22	5.63	2.80	1.22	**4.01**
		b	11.51	5.89	2.82	1.47	
		c	10.19	5.37	2.76	1.46	
	10% Power mismatch	a	7.07	7.34	3.64	2.01	**4.07**
		b	13.56	6.69	3.49	1.84	
		c	13.97	7.51	3.76	1.93	
	80% Power mismatch	a	10.03	5.61	2.77	1.51	**4.12**
		b	11.52	5.71	2.80	1.51	
		c	10.05	5.53	2.82	1.46	
Non-Islanding	Load switching at DG-1	a	1.81	0.96	0.50	0.25	0.55
		b	1.93	1.03	0.52	0.26	
		c	1.84	0.94	0.47	0.23	
	DG-1 tripped	a	1.84	0.92	0.46	0.24	0.56
		b	1.82	0.93	0.48	0.25	
		c	1.96	1.02	0.51	0.26	

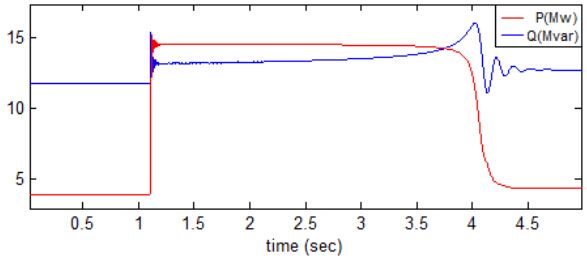

Fig. 12. Active and reactive power changes at PCC by motor starting.

Table 6. ***Effective singular values and WSEI for reactive power mismatch during islanding and non-islanding conditions at target DG-4 [46] .***

EVENTS		Phase	λ_1	λ_2	λ_3	λ_4	WSEI
Islanding	0% Power mismatch	a	12.60	6.69	3.47	1.76	**4.02**
		b	13.44	7.24	3.66	1.83	
		c	12.13	5.87	3.15	2.18	
	10% Power mismatch	a	13.44	7.42	3.96	1.87	**4.17**
		b	13.62	6.84	3.49	1.83	
		c	12.82	6.34	3.07	2.08	
	60% Power mismatch	a	14.88	7.93	4.11	2.17	**4.35**
		b	14.88	7.59	3.80	2.12	
		c	13.98	6.97	3.49	2.10	
Non-Islanding	Load switching at DG-1	a	1.83	0.97	0.50	0.25	0.55
		b	1.96	1.05	0.53	0.26	
		c	1.88	0.96	0.48	0.23	
	DG-1 tripped	a	1.85	0.94	0.45	0.23	0.55
		b	1.77	0.94	0.45	0.24	
		c	1.95	1.04	0.50	0.26	

Table 7. ***Disturbance classification accuracy [47].***

Disturbances	S-Transform	EMD-HT
Harmonic	88	95.75
Flicker	90	98
Sag with Harmonic	91.37	98
Swell with Harmonic	87.18	91.45
Momentary Interruption	99	100
Oscillatory Transient	98	100
Impulsive Transient	95.12	100
Notches	96	100
Overall Accuracy	93.08	97.9

Table 8. ***Comparison with other methods [47].***

Method	Classification Accuracy
Wavelet transform and neural network	94.37
Neural network	95.93
Wavelet transform and neural fuzzy	96.50
Wavelet packet and support vector machines	97.25
Proposed method	97.9

6. CONCLUSION

In this article a time-frequency transform based on EMD-HT is recommended as a new passive islanding detection method. EMD-HT is a promising new addition to existing tool for nonlinear and non-stationary signal processing. The reported results at this article and other articles represent new insights on EMD and its use.

Some methods are unable to detect islanding events when the power mismatch decreases during islanding and have a large Non Detection Zone (NDZ) such as ROCOF and dv/dt relay that in power mismatch less than 15%, have false operation. The proposed method has a zero NDZ and the relay performance is independent from the power imbalance. Speed is another important function for an anti-islanding relay that in this method the time response is less than one cycle. The reason of the success of this method is that the analysis of transient signals in the time-frequency domain is used.

The proposed method could overcome on the weaknesses of other methods. Now we have a relay that includes advantages: more accuracy, lower cost, without inject perturbation to the network, supporting non-linear and non-stationary and discrete signals, without classifier and network training, higher speed and simple computations that can be online. Also, because the proposed method uses energy spectrum index, so it is suitable for both synchronous and inverter based DGs. Since the proposed method is simple and is based on EMD-HT, it can be easily implemented on the DSP/FPGA board for developing the anti-islanding relay module.

REFERENCES

[1] A.M.Massoud, K. H. Ahmed, S. J. Finney, and B.W.Williams, "Harmonic distortion-based island detection technique for inverter-based distributed generation," IET Renew. Power Gener., vol. 3, no. 4, pp.493–507, Dec. 2009.

[2] A. Samui and S. R. Samantaray, "Assessment of ROCPAD relay for islanding detection in distributed generation," IEEE Trans. Smart Grid,vol. 2, no. 2, pp. 391–398, Jun. 2011.

[3] TUNLASAKUN K., KIRTIKARA K., THEPA S., MONYAKUL V.:'CPLD-based islanding detection for mini grid connected inverter in renewable energy'. IEEE TENCON Conf., vol. 4, pp. 175–178, November 2004.

[4] FREITAS W., XU W., AFFONSO C.M., HUANG Z.: 'Comparative analysis between ROCOF and vector surge relays for distributed generation applications', IEEE Trans. Power Deliv., 20, (2), pp. 1315–1324, 2005.

[5] FLORIO A., MARISCOTTI A., MAZZUCCHELLI M.: 'Voltage sag detection based on rectified voltage processing', IEEE Trans. Power Deliv., 19, (4), pp. 1962–1967, 2004.

[6] DE MANGO F., LISERRE M., AQUILA A.D.: 'Overview of anti-islanding algorithms for PV systems. Part II: active methods'. IEEE Power Electronics and Motion Control Conf., pp. 1884–1889, January 2007.

[7] REDFERNM.A., USTA O., FIELDING G.: 'Protection against loss of utility grid supply for a dispersed storage and generation unit', IEEE Trans. Power Deliv., 8, (3), pp. 948–954, 1993.

[8] VIEIRA J.C.M., FREITAS W., XU W., MORELATO A.: 'Efficient coordination of ROCOF and frequency relays for distributed generation protection by using the

application region', IEEE Trans. Power Deliv., 21, (4), pp. 1878–1884, 2006.

[9] MOORE P.J., ALLMELING J.H., JOHNS A.T.: 'Frequency relaying based on instantaneous frequency measurement [power systems]', IEEE Trans. Power Deliv., 11,(4),pp. 1737–1742, 1996.

[10] AFFONSO C.M., FREITAS W., XU W., DA SILVA L.C.P.: 'Performance of ROCOF relays for embedded generation applications', IEEE Gener. Transm. Distrib., 152, (1), pp. 109–114, 2005.

[11] VIEIRA J.C.M., FREITAS W., HUANG Z., XU W., MORELATO A.: 'Formulas for predicting the dynamic performance of ROCOF relays for embedded generation applications', IEE Proc. Gener. Transm. Distrib., 153, (4), pp. 399–406, 2006.

[12] SHYH-JIER H., FU-SHENG P.: 'A new approach to islanding detection of dispersed generators with self-commutated static power converters', IEEE Trans. Power Deliv.,15, (2), pp. 500–507, 2000.

[13] SALMAN S.K., KING D.J., WELLER G. 'New loss of mains detection algorithm for embedded generation using rate of change of voltage and changes in power factors'. IEE Developments in Power System Protection Conf.,pp. 82–85, 2001.

[14] BRIGHT C.G.: 'COROCOF: comparison of rate of change of frequency protection. A solution to the detection of loss of mains'. IEE Developments in Power System Protection Conf., pp. 70–73, 2001.

[15] SINGAM B., HUI L.Y.: 'Assessing SMS and PJD schemes of anti-islanding with varying quality factor'. IEEE Power and Energy Conf., pp. 196–20, November 2006.

[16] JANG S.-I., KIM K.-H.: 'An islanding detection method for distributed generations using voltage unbalance and total harmonic distortion of current', IEEE Trans. Power Deliv., 19, (2), pp. 745–752,2004.

[17] MENON V., NEHRIR M.H.: 'A hybrid islanding detection technique using voltage unbalance and frequency set point', IEEE Trans. Power Syst., 22, (1), pp. 442–448, 2007.

[18] VIEIRA J.C.M., FREITAS W., HUANG Z., XU W., MORELATO A.: 'Formulas for predicting the dynamic performance of ROCOF relays for embedded generation applications', IEE Proc. Gener. Transm. Distrib., 153, (4), pp. 399–406, 2006.

[19] FREITAS W., HUANG Z., XU W.:'A practical method for assessing the effectiveness of vector surge relays for distributed generation applications', IEEE Trans. Power Deliv., 20, (1), pp. 57–63, 2005.

[20] FREITAS W., XU W.: 'False operation of vector surge relays', IEEE Trans. Power Deliv., 19, (1), pp. 436–438, 2004.

[21] LISERRE M., BLAAGJERG F., TEODORESCU R.: 'Grid impedance detection via excitation of LCL-filter resonance'. IEEE Industry Applications Conf., vol. 2,pp. 910–916, October 2005.

[22] ROPP M., GINN J., STEVENS J., BOWER W., GONZALEZ S.:'Simulation and experimental study of the impedance detection anti-islanding method in the single-inverter case'. IEEE Photovoltaic Energy Conversion Conf., vol. 2, pp. 2379–2382, May 2006.

[23] BERTLING F., SOTER S.: 'A novel converter integrable impedance measuring method for islanding detection in grids with widespread use of decentral generation'. IEEE Power Electronics, Electrical Drives, Automation and Motion Conf., pp. 503–507, May 2006.

[24] SINGAM B., HUI L.Y.: 'Assessing SMS and PJD schemes of anti-islanding with varying quality factor'. IEEE Power and Energy Conf., pp. 196–201, November 2006.

[25] HUNG G.-K., CHANG C.-C., CHEN C.-L.: 'Automatic phase-shift method for islanding detection of grid-connected photovoltaic inverters', IEEE Trans. Energy Convers.,18, (1), pp. 169–173, 2003.

[26] LOPES L.A.C., HUILI S.: 'Performance assessment of active frequency drifting islanding detection methods', IEEE Trans. Energy Convers., 21, (1), pp. 171–180, 2006.

[27] BERTLING F., SOTER S.: 'A novel converter integrable impedance measuring method for islanding detection in grids with widespread use of decentral generation'. IEEE Power Electronics, Electrical Drives, Automation and Motion Conf., pp. 503–507, May 2006.

[28] [28] JUNG Y., CHOI J., YU B., SO J., YU G.: 'A novel active frequency drift method of islanding prevention for the grid-connected photovoltaic inverter'. IEEE Power Electronics Specialists Conf., pp. 1915–1921, 2005.

[29] ROPP M.E., BEGOVIC M., ROHATGI A.: 'Analysis and performance assessment of the active frequency drift method of islanding prevention', IEEE Trans. Energy Convers., 14, (3), pp. 810–816, 1999.

[30] LOPES L.A.C., HUILI S.: 'Performance assessment of active frequency drifting islanding detection methods', IEEE Trans. Energy Convers., 21, (1), pp. 171–180, 2006.

[31] SINGAM B., HUI L.Y.: 'Assessing SMS and PJD schemes of anti-islanding with varying quality factor'. IEEE Power and Energy Conf., pp. 196–201, November 2006.

[32] SMITH G.A., ONIONS P.A., INFIELD D.G.: 'Predicting islanding operation of grid connected PV inverters', IEE Electr. Power Appl., 147, (1), pp. 1–6, 2000.

[33] JEONGJ.B., KIMH.J., AHNK.S., KANGC.H.: 'A novel method for anti-islanding using reactive power'. IEEE Telecommunications Conf., pp. 101–106, September 2005.

[34] JERAPUTRA C., ENJETI P.N.: 'Development of a robust anti-islanding algorithm for utility interconnection of distributed fuel cell powered generation', IEEE Trans.Power Electron., 19, (5), pp. 1163–1170, 2004.

[35] ROPP M.E., BEGOVIC M., ROHATGI A., KERN G.A., BONN R.H. SR., GONZALEZ S.: 'Determining the relative effectiveness of islanding detection methods using phase criteria and non detection zones', IEEE Trans. Energy Convers., 15, (3), pp. 290–296, 2000.

[36] LOPES L.A.C., HUILI S.: 'Performance assessment of active frequency drifting islanding detection methods', IEEE Trans. Energy Convers., 21, (1), pp. 171–180, 2006.

[37] WANG X., FREITASW., XUW., DINAVAHI V.: 'Impact of DG interface controls on the SANDIA frequency shift anti-islanding method', IEEE Trans. Energy Convers., 22, (3), pp. 792–794, 2007.

[38] ROBITAILLE M., AGBOSSOU K., DOUMBIA M.L.: 'Modeling of an islanding protection method for a hybrid renewable distributed generator', Electr. Comput. Eng., 1,pp. 1477–1481, 2005.

[39] HERNANDEZ-GONZALEZ G., IRAVANI R.: 'Current injection for active islanding detection of electronically-interfaced distributed resources', IEEE Trans. Power Deliv., 21,(3), pp. 1698–1705, 2006.

[40] N. W. A. Lidula, Student Member, IEEE, and A. D. Rajapakse, Senior Member, IEEE "A Pattern Recognition Approach for Detecting Power Islands Using Transient Signals—Part I: Design and Implementation" IEEE TRANSACTIONS ON POWER DELIVERY, VOL. 25, NO. 4, OCTOBER 2010.

[41] S.R. Samantaray , A. Samui , B. Chitti Babu "Time-frequency transform-based islanding detection in distributed generation" IET Renew. Power Gener., Vol. 5, Iss. 6, pp. 431–438 doi: 10.1049/iet-rpg.2010.0166, 2011.

[42] Ming-Huan Lee; Kuo-Kai Shyu; Po-Lei Lee; Chien-Ming Huang; Yun-Jen Chiu; ,

"Hardware Implementation of EMD Using DSP and FPGA for Online Signal Processing," Industrial Electronics, IEEE Transactions on , vol.58, no.6, pp.2473-2481, June 2011.

[43] Stuti Shukla, S. Mishra and Bhim Singh, "Empirical-Mode Decomposition with Hilbert Transform for Power-Quality Assessment", IEEE Transactions on Power Delivery, Vol. 24, No. 4, October 2009.

[44] S.L. Hahn, Hilbert Transforms in Signal Processing, Artech House, Boston, London, 1996.

[45] Wang Qinghao; Wang Tianshi; Sheng Jidong; Zhang Xinwei; Shi Guodong; , "The power quality disturbance detection and classification method based on EMD," Innovative Smart Grid Technologies - Asia (ISGT Asia), 2012 IEEE , vol., no., pp.1-3, 21-24 May 2012.

[46] Ankita Samui, Student Member, IEEE, and S. R. Samantaray, Senior Member, IEEE, "Wavelet Singular Entropy-Based Islanding Detection in Distributed Generation" , IEEE Transactions on Power Delivery, Vol. 28, No. 1, January 2013.

[47] B. Biswal, Member, IEEE, M. Biswal, Member, IEEE, S. Mishra, Senior Member, IEEE and R. Jalaja,Student Member, IEEE, "Automatic Classification of Power Quality Events Using Balanced Neural Tree" , Manuscript received July 24, 2012. Accepted for publication February 8, 2013.